International Forum on Aeroelasticity and Structural Dynamics
IFASD 2017
25-28 June 2017 Como, Italy

FREE-VIBRATION ANALYSIS OF TAPERED WING STRUCTURES USING REFINED ONE-DIMENSIONAL MODELS

A. Viglietti[1], **E. Zappino**[1], **E. Carrera**[1]

[1]Politecnico di Torino, Mechanical and Aerospace Engineering Dept.
Turin, Italy
andrea.viglietti@polito.it
enrico.zappino@polito.it
erasmo.carrera@polito.it

Keywords: CUF, one dimensional, tapered, thin-walled, free-vibration.

Abstract: This work presents results from free-vibration analyses on tapered wing box made of composite material. The analyses are performed through a refined one-dimensional model based on the Carrera Unified Formulation. The displacements over the beam cross-section are evaluated using polynomial expansions. In this way, no geometrical approximations are introduced in the problem and a three-dimensional result can be obtained. Two simple tapered wing boxes have been considered and different laminations have been taking into account. The results are compared with a shell model achieved by a commercial code. The results demonstrate the good accuracy of the model and his use in tailoring analyses.

INTRODUCTION

In the aeronautical field, due to their rigid requirements regarding weight and stiffness, the tapered thin-walled structures are widely used. Thanks to their proprieties and the materials which they are made of, these structures provide a high stiffness/mass ratio and make them attractive. Tapered beams are investigated with different methods. Assuming that stiffness coefficients are a function of the beam axis, the classical theories, such as Eulero-Bernulli [1], provide not accurate results due to their assumption even if, ensure a low computational cost. Cicala [2] and Timoshenko-Goodier [3] proposed analytical methods which include the shear stress giving more accurate results. An easy way to analyze tapered beam concerns the use of several rigidly joined prismatic sections to approximate the tapered shape. The accuracy of the results increases with the number of subdivisions. An example of this stepped of piece-wise approach can be found in work by Ji Yao Shen et al.. [4]. With the introduction of the Finite Element Methods by Turner et al. [5] new approaches have emerged. As before said, the thin-walled structure, TWS, are very attractive for the aeronautical application. Typical TWS have closed cross-section make them good structures to deal with bending and torsional loads. Their complex behavior and the non-classical geometries such as tapered shape, make the classical theories incapable for analysing this topic providing accurate results. Some works about the extension of the classical theories are proposed by Bruhn [6] or Vlasov [7]. The Carrera Unified Formulation (CUF) presented by Carrera et al. [8] is an advanced numerical tool which allows 1-D, 2-D and 3-D refined structural models to be derived in a compact form. Different classes of refined one-dimensional models have been obtained in the past years. The 1-D CUF models are able to describe 3-D problems without introducing geometrical approximations. Through

different types of expansion polynomials, these models approximate the cross-sectional displacements. The first class of models is represented by the TE model which uses the Taylor Polynomials to describe the cross-section. The work by Carrera et al.. [9] about this topic is suggested. More recently the Lagrange polynomials are introduced to describe the displacement field over the beam cross-section as presented by Carrera and Petrolo [10]. Other classes of models have been proposed using other expansions such as Carrera et al. [11]. This work has the aim to explore the capabilities of a refined 1-D Finite Element model based on CUF for the free-vibration analysis of tapered structures made of composite material . This paper is subdivided into two main parts. The first part concerns the mathematical approach and the second part investigates the modal behavior of two tapered boxes. In the end, some conclusions are listed.

BEAM PRESENT MODEL

In this section, an overview of the mathematical approach used in this work is introduced. The first part concerns the explanation of the basis to define the displacement, stress and strain fields. After some preliminaries, the Carrera Unified Formulation for 1-D models is presented followed by the FEM solution which is used to solve the problem.

Preliminaries

Using the present 1-D model, a multi-component structure can be described at element level with several beam formulations. The structure is oriented respect a global reference frame (x_G, y_G, z_G). Each beam formulation used to describe the structure or a component, is referred to its own local reference system (x, y, z). This last frame can be translated and rotated respect the global one. y is the local beam axis while x, z is the plane where the beam cross-section lies. These frames are figured in Figure 1.

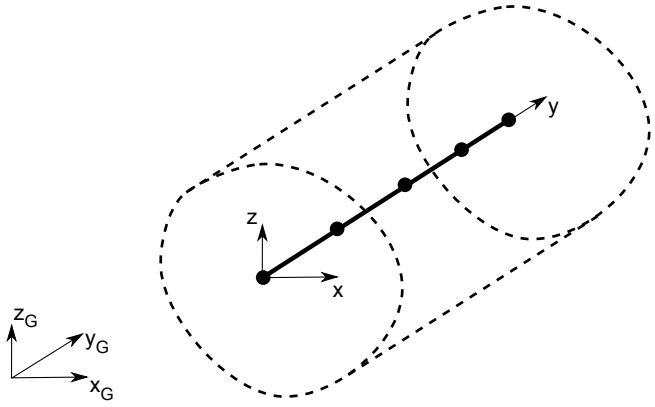

Figure 1: Reference system representation.

Each point has a local displacement vector $\boldsymbol{u}$ defined as:

$$\boldsymbol{u}^T(x, y, z) = \{u_x \, u_y \, u_z\} \tag{1}$$

The strain $\boldsymbol{\epsilon}$ and the stress vector $\boldsymbol{\sigma}$ can be written as follows:

$$\boldsymbol{\sigma}^T(x, y, z) = \{\sigma_{xx}, \sigma_{yy}, \sigma_{zz}, \tau_{xy}, \tau_{xz}, \tau_{yz}\} \tag{2}$$

$$\boldsymbol{\epsilon}^T(x,y,z) = \{\epsilon_{xx}, \epsilon_{yy}, \epsilon_{zz}, \epsilon_{xy}, \epsilon_{xz}, \epsilon_{yz}\} \tag{3}$$

To define the geometrical relations the differential operator $\boldsymbol{b}$ (a 6×3 matrix) is introduced to obtain the following linear strain-displacement relation:

$$\boldsymbol{\epsilon} = \boldsymbol{bu} \tag{4}$$

The explicit formulation can be found in the book by Carrera *et al.* [8].

Using the linear form of the Hooke's law, the stress vector is obtained as:

$$\boldsymbol{\sigma} = \boldsymbol{C\epsilon} \tag{5}$$

Here, $\boldsymbol{C}$ is the 6×6 *material stiffness matrix*. It contains the elastic coefficients and it is referred to a material reference system $(1, 2, 3)$. The material properties can be arbitrarily rotated of an angle θ around the axis 1 that correspond with the z-direction. When $\theta = 0$ the longitudinal direction of the material corresponds with the beam axis. The problem is represented in fig.2.

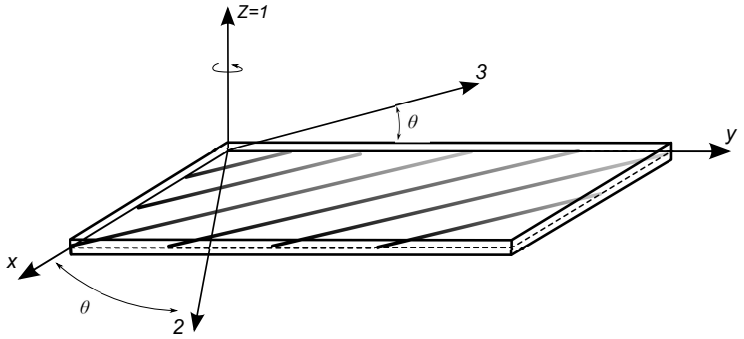

Figure 2: Material reference system.

$\boldsymbol{C}$ is a symmetric matrix, then $C_{ij} = C_{ji}$. It is composed by 21 independent elastic coefficients if a *anisotropic* material is considered. If an *orthotropic* material is considered, the coefficients are reduced to 9 components. Other information about this topic such as the explicit form of $\boldsymbol{C}$ can be found in the books by Tsai [12] or Reddy [13]. Having regard to the possibility of having an arbitrary direction of the material frame, a transformation matrix $\boldsymbol{T}$ is introduced as follows:

$$\boldsymbol{T} = \begin{bmatrix} cos^2\theta & sin^2\theta & 0 & 0 & 0 & sin2\theta \\ sin^2\theta & cos^2\theta & 0 & 0 & 0 & -sin2\theta \\ 0 & 0 & 1 & 0 & 0 & 0 \\ 0 & 0 & 0 & cos\theta & -sin\theta & 0 \\ 0 & 0 & 0 & sin\theta & cos\theta & 0 \\ -cos\theta sin\theta & cos\theta sin\theta & 0 & 0 & 0 & cos^2\theta - sin^2\theta \end{bmatrix} \tag{6}$$

A *transformed material stiffness matrix* $\tilde{\boldsymbol{C}}$ is introduced and it is obtained as

$$\tilde{\boldsymbol{C}} = \boldsymbol{TCT^T} \tag{7}$$

After that, the Hooke's law can be re-written

$$\boldsymbol{\sigma} = \tilde{\boldsymbol{C}}\boldsymbol{\epsilon} \tag{8}$$

If the material has the same behavior in all directions, it is a *isotropic* material. In this case, there is no need to define a material reference system and a rotation matrix. The performance of the material can be described with only one value of the Poisson ratio and of Young's modulus. These assumptions lead to have

$$C_{11} = C_{22} = C_{33} \qquad C_{12} = C_{13} = C_{23} \qquad C_{44} = C_{55} = C_{66} \tag{9}$$

Cross-sectional kinematic approximation

In the beam models based on the Carrera Unified Formulation, the displacement field $\boldsymbol{u}$ can be written as the product of two terms. The first term describes the displacement field over the cross-section while the second one along the beam axis. The displacement field can be write through the following form:

$$\mathbf{u}(x, y, z) = F_\tau(x, z)\mathbf{u}_\tau(y), \qquad \tau = 1, 2 \dots M, \tag{10}$$

where $\mathbf{u}_\tau$ is the displacement vector, F_τ represents a function expansion used to approximate the behavior of the beam cross-section. M is the number of the expansion terms. The present work uses the Lagrange polynomials to describe the beam cross-section with high-order elements. The Lagrange Elements introduce as unknowns only translational displacements. In this way, an accurate description of the cross-section geometry is possible and a 3-D description of the structure behaviour can be achieved. Several sets of Lagrange Elements, more or less refined, are available. More details can be found in [14] or [8]. If a nine-point element (L9) is used over the cross-section, the formulation of the displacement becomes:

$$\begin{aligned} u_x &= F_1 u_{x_1} + F_2 u_{x_2} + F_3 u_{x_3} \dots + F_9 u_{x_9} \\ u_y &= F_1 u_{y_1} + F_2 u_{y_2} + F_3 u_{y_3} \dots + F_9 u_{y_9} \\ u_z &= F_1 u_{z_1} + F_2 u_{z_2} + F_3 u_{z_3} \dots + F_9 u_{z_9} \end{aligned} \tag{11}$$

where $u_{x_1} \dots u_{x_9}$ represent the components x of the displacement field of each node of the L9 element.

Finite Element formulation

The Finite Element model is used to solve the one-dimensional problem. Introducing the shape functions N_i the vector $\boldsymbol{u}$ can be written as

$$\mathbf{u}(x, y, z) = F_\tau(x, z)N_i(y)\mathbf{u}_{\tau i} \tag{12}$$

where $\mathbf{u}_{\tau i}$ is the nodal displacements vector. The index i indicates the i^{th} node of the beam element. The used shape functions are reported in [8]. The governing equations can be achieved

using the PVD (Principle of Virtual Displacements). It is expressed with the following form where the term δ denotes the virtual variation:

$$\delta L_{int} = -\delta L_{ine} \tag{13}$$

The two member of 13 can be written as follow:

$$\delta L_{int} = \int_V \delta \boldsymbol{\epsilon}^T \boldsymbol{\sigma} dV \tag{14}$$

$$\delta L_{ine} = \int_V \delta \boldsymbol{u}^T \rho \ddot{\boldsymbol{u}} dV \tag{15}$$

From 14 and 15 the stiffness matrix $\boldsymbol{K}$ and the mass matrix $\boldsymbol{M}$ are obtained in terms of *fundamental nucleus* (*FN*), a 3x3 block with fixed form. Its components are reported in [15]. A complete description of the FN derivation and its use to achieve the global matrices are presented in [8].

Knowing the form of $\boldsymbol{K}$ and $\boldsymbol{M}$, the 13 can be rewritten as follows:

$$\boldsymbol{M}\ddot{\boldsymbol{u}} + \boldsymbol{K}\boldsymbol{u} = 0 \tag{16}$$

that is the undamped dynamic problem. Considering harmonic solutions and using the classical eigenvalue problem, the natural frequencies ω_k can be obtained.

$$(-{\omega_k}^2 \boldsymbol{M} + \boldsymbol{K})\boldsymbol{u_k} = 0 \tag{17}$$

where $\boldsymbol{u_k}$ is the *k*th eigenvector.

Rotation and Assembling Procedure

Each beam description can be rotated and translated in the space. In this way, by imposing the congruence of the displacements in some nodes defined by the geometry, a complex structure can be obtained. For more details, [16] is proposed.

RESULTS

Two wing boxes are presented in this section. The two structures are made of *CFRP: Carbon Fiber Reinforced Polymer*. This composite has the following proprieties: $E_{LL} = 50e9\ Pa$, $E_{TT} = E_{ZZ} = 10e9\ Pa$, $G = 5e9\ Pa$, Poissons's ratio $\nu = 0.25$ and density of $1700\ kg/m^3$. E_{LL} is referred to the fiber direction. Each structure is characterized with a 2-ply laminate. The laminate will be defined from the inner layer to the external one. If a lamination of '$90°/0°$' is considered, it identifies the inner layer with fibers rotated of 90-degree respect the X_{m0}-axis and, the external one, with no rotation. The results are compared with results obtained from shell models achieved by the commercial code NASTRAN. The CQUAD elements are used to describe the structures.

Tapered box with no sweep angle

Here, the tapered box shown in 3 is investigated. The box is simplified using only four panels to describe the geometry. The structure has the following dimensions: $L = 2$, $H_1 = 0.22$, $H_2 = 0.12$, $R_1 = 0.42$ and $R_2 = 0.2$. The dimensions are expressed in $metres$. The thickness of the laminate is equal to $1\ cm$ in order to avoid the presence of many shell-like modal shapes. In this way, the presence of global modes is facilitated. Each layer is composed of the orthotropic material before introduced. The structure is described using the layer-wise approach. In this way a three node beam element is used to describe each layer as a separated component, for a total of eight beam element. The B3 elements are placed over the thickness of the layer. The Lagrange polynomials are used to describe the cross-section of the beam, so in this case, the tapered shape of the panel. More details about the use of Lagrange elements and the use of the present formulation to describe tapered structure is given in [16]. Figure 3*a* shows the description used in the corners.

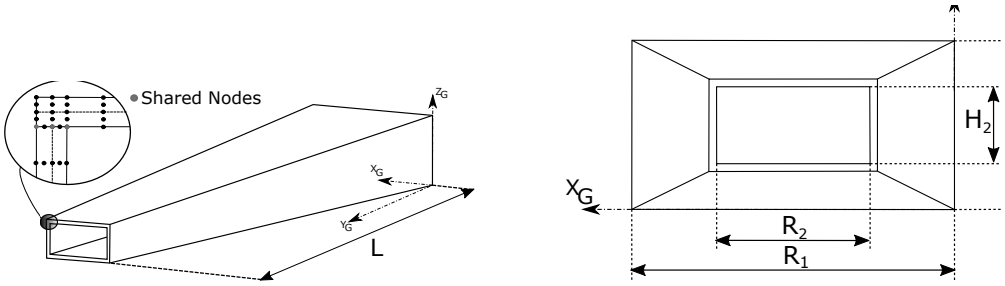

(a) (b)

Figure 3: Tapered Box with no sweep angle.

Figure 4 shows the fiber direction (X_m-*axis*) of the panels. The fiber will be rotated of an angle equal to θ respect X_{m0}-*axis*. For each panel the positive rotation of the fiber are made considering the Z_m-*axis* perpendicular to the panel and oriented towards the outside of the structure.

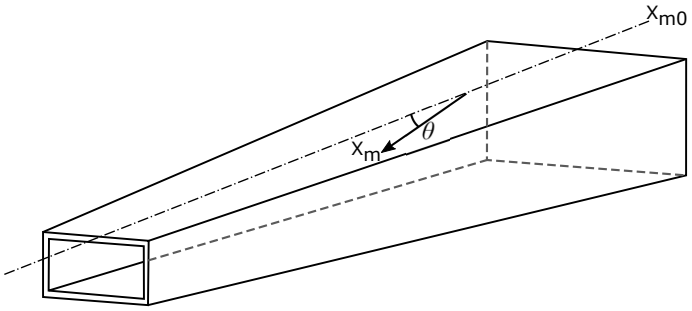

Figure 4: Fiber direction.

Table 1 shows the first ten modes obtained with the present model. Three laminations are take into account: $90°/0°$, $60°/-30°$ and $45°/-45°$. The first angle of the lamination is referred to the internal layer. The frequencies obtained from the present model show a good correspondence with those obtained from the commercial code. Figure 5 shows the modal shapes of the mode 3,8 and 9 with the three laminations considered.

Using the first lamination, the modal shapes are well defined. The first two frequencies are pure bending mode in the plane yz and in plane xy. The next bending modes are characterized by a shell-like behavior of the horizontal panels. This can be see in 5*a*. Then, the model detects

	Mode 1	Mode 2	Mode 3	Mode 4	Mode 5	Mode 6	Mode 7	Mode 8	Mode 9	Mode 10
$90°/0°$ lamination	(b_{yz})	(b_{xy})	(b_{yz}, s)	(s)	(t)	(s)	(b_{yz}, s)	(s)	(t)	(b_{yz}, s)
Present Model	56,24	90,23	181,53	192,64	196,09	235,62	240,47	278,89	282,68	292,42
Nastran Shell	56,00	90,09	174,50	182,82	192,46	222,06	221,65	260,48	278,52	266,88
$60°/-30°$ lamination	(b_{yz}, b_{xy})	(b_{xy}, b_{yz})	(b_{yz}, s, b_{xy})	(s, t)	(t)	(s, t)	(b_{yz}, s, b_{xy})	(s, t)	(s, t)	(b_{yz}, s, b_{xy})
Present Model	44,63	72,67	175,41	183,05	194,12	229,64	232,35	272,55	278,38	286,11
Nastran Shell	44,39	72,33	168,70	173,30	188,82	216,47	213,18	268,35	256,58	261,97
$45°/-45°$ lamination	(b_{yz})	$(b_{xy}))$	(b_{yz}, s)	(s)	(t)	(s)	(b_{yz}, s)	(t)	(s, t)	(b_{yz}, s)
Present Mode	41,93	68,70	170,48	179,56	188,33	226,56	230,67	269,79	272,24	288,60
Nastran Shell	41,72	68,37	164,29	169,89	182,26	213,63	210,91	260,16	255,00	262,47

Note: b=Bending Mode, t=Torsional Mode, s: Shell-Like Mode. The bending modal shapes are divided in bending mode in the plane yz and in the plane xy.

Table 1: First 10 modes of the tapered box with no sweep angle with different laminations. The results are obtained from the present model (11844 Dofs) and from the Shell model(150000 Dofs).

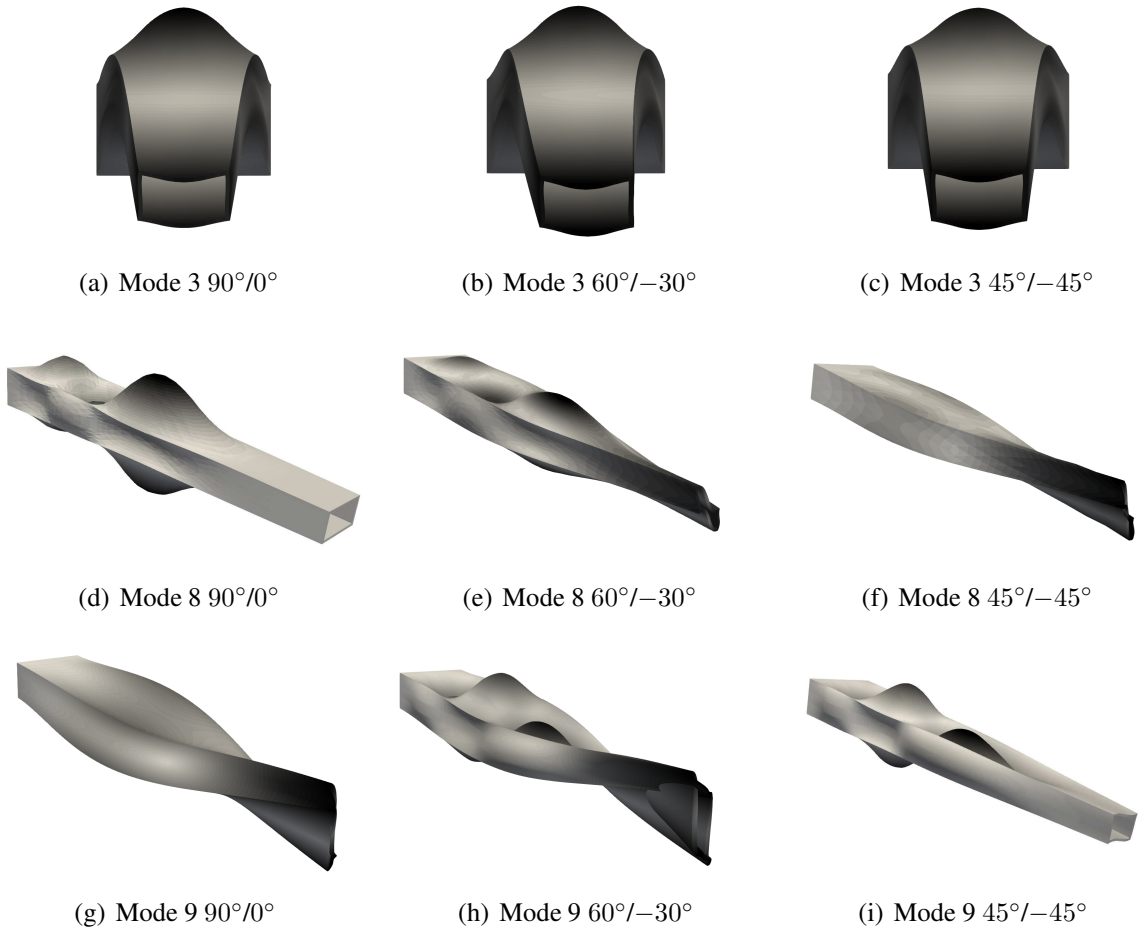

(a) Mode 3 $90°/0°$ (b) Mode 3 $60°/-30°$ (c) Mode 3 $45°/-45°$

(d) Mode 8 $90°/0°$ (e) Mode 8 $60°/-30°$ (f) Mode 8 $45°/-45°$

(g) Mode 9 $90°/0°$ (h) Mode 9 $60°/-30°$ (i) Mode 9 $45°/-45°$

Figure 5: Modal shapes of the mode 3,8 and 9 with different lamination.

three pure shell-like modes and two pure torsional modes. Introducing the second lamination, the present model correctly provides the alteration of the modal shapes. A coupling effect between the two bending behaviors can be noted in the figure 5*b*. A coupling torsional effect can also be individuated in the shell-like modes. With the third lamination, these effects become weaker, and the modal shapes are very similar to those of the first case. On the contrary, mode 9 and mode 10 are more influenced, and the alteration of the modal behavior is shown in 5.

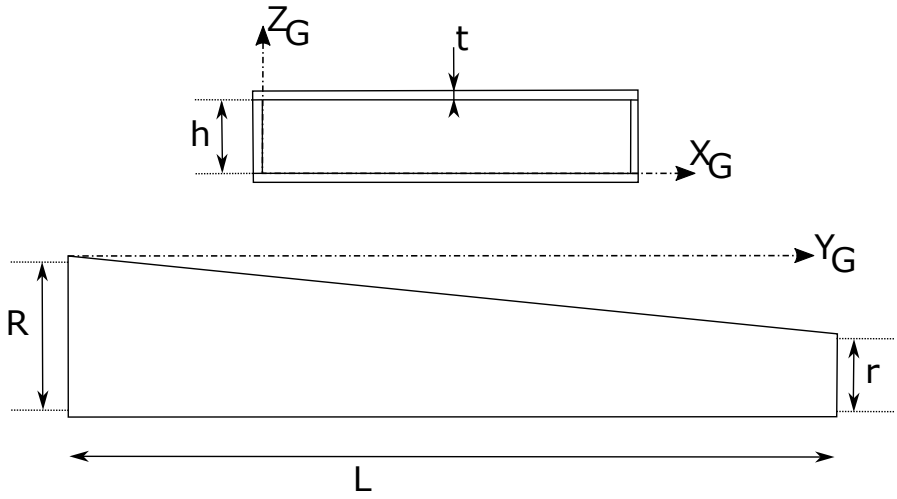

Figure 6: Tapered Box with sweep angle.

Wing box with tapered edge and sweep angle.

The second structure represents a tapered wing box with a sweep angle and no variation in the box thickness. The geometry are shown in figure 6 and the geometrical characteristics are the following: $L = 2\ m$, $R = 0.4\ m$, $r = 0.2\ m$, $h = 0.08\ m$ and $t = 0.01\ m$. The structure is made of the same previous laminate, and the same description at the corners is introduced. In this problem, the first four modes are investigated varying the lamination in a range of $180°$. An angle of $90°$ is maintained between the two layers. The orientation frames of the material are the same introduced in the previous case. In some points, the results are compared with those provided by the Nastran Shell Model. The degrees of freedom of this case is equal to those of the previous case.

The figure 7 shows the behavior of the first four modes. The lamination changes from $90°/0°$ to $-90°/-180°$. As the graph shows, the bending modes are characterized by the lowest frequency with a lamination of $45°/-45°$. In this case, there is no fiber parallel to the wingspan (or no fiber parallel to the chord direction). On the contrary, for the torsional mode the highest frequencies are obtained with the $45°/-45°$ lamination, as shown in figure 7*d*. In the control points, the frequencies are very close to those obtained from the commercial code and, the present model introduces an average error less than 5%.

Figure 8 shows the deformation at the tip in the first three modes in the first half of the range. From the previous pictures can be noted that in this case the behavior is symmetric. Figure 8*a* and figure 8*b* show the effects of the lamination in the first bending mode. The range of lamination is subdivided in two figure for a better representation. Due to the sweep angle, in the first bending mode with $90°/0°$ lamination a torsional effect can be noted. The torsional effect is deleted if the lamination is shifted to $45°/-45°$ Figure 8*b* represents the second range of the laminations. Can be noted the slight difference in the deformation between $90°/0°$ and $0°/-90°$. Figure 8*c* shows the deformation of the second mode. The coupling with a bending effect on the plane *yz* can be appreciated. Figure 8*d* represents the deformation in the third bending mode. A shell-effect can be noted on the top and bottom panels. In this case, a bending effect on the plane *xy* is added at the global deformation. In the second and third mode, the lamination $90°/0°$ and $0°/-90°$ are not reported because the results are very close to those with a $45°/-45°$ lamination and they would be confused on the pictures.

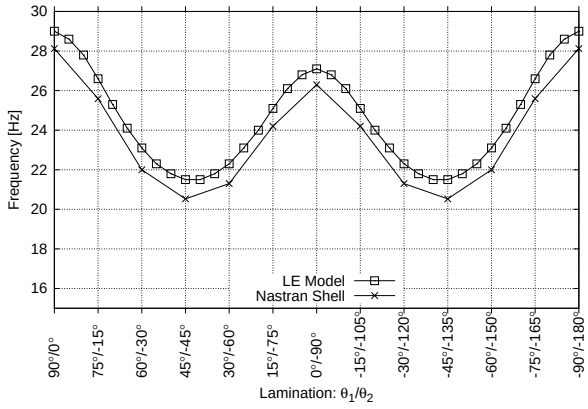

(a) 1^{st} Mode: Bending *xz-plane*

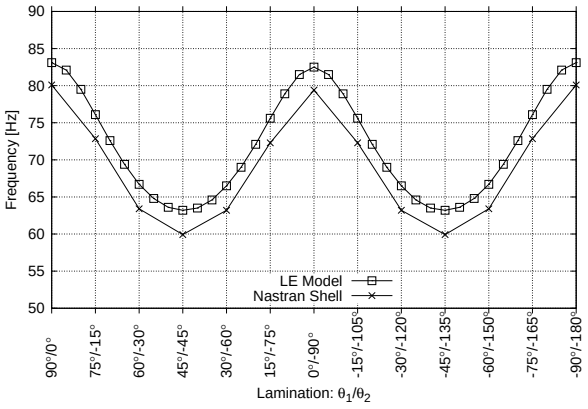

(b) 2^{nd} Mode: Bending *xy-plane*

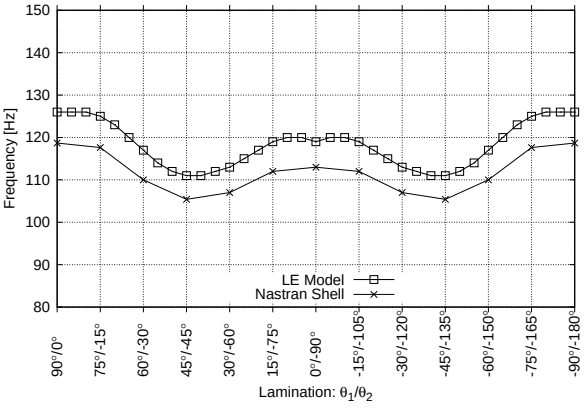

(c) 3^{rd} Mode: Bending *xz-plane*+Shell-like

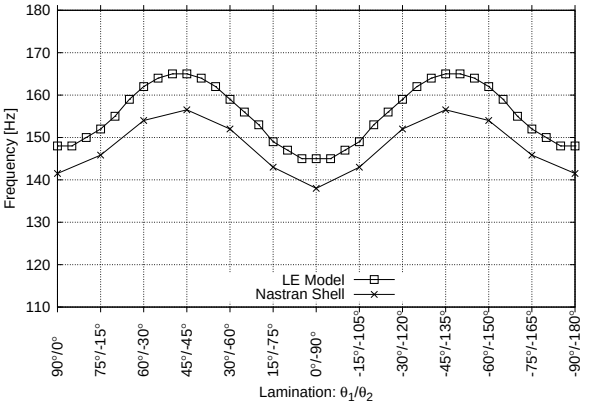

(d) 4^{th} Mode: Torsional

Figure 7: Comparison of the first 4 modes.

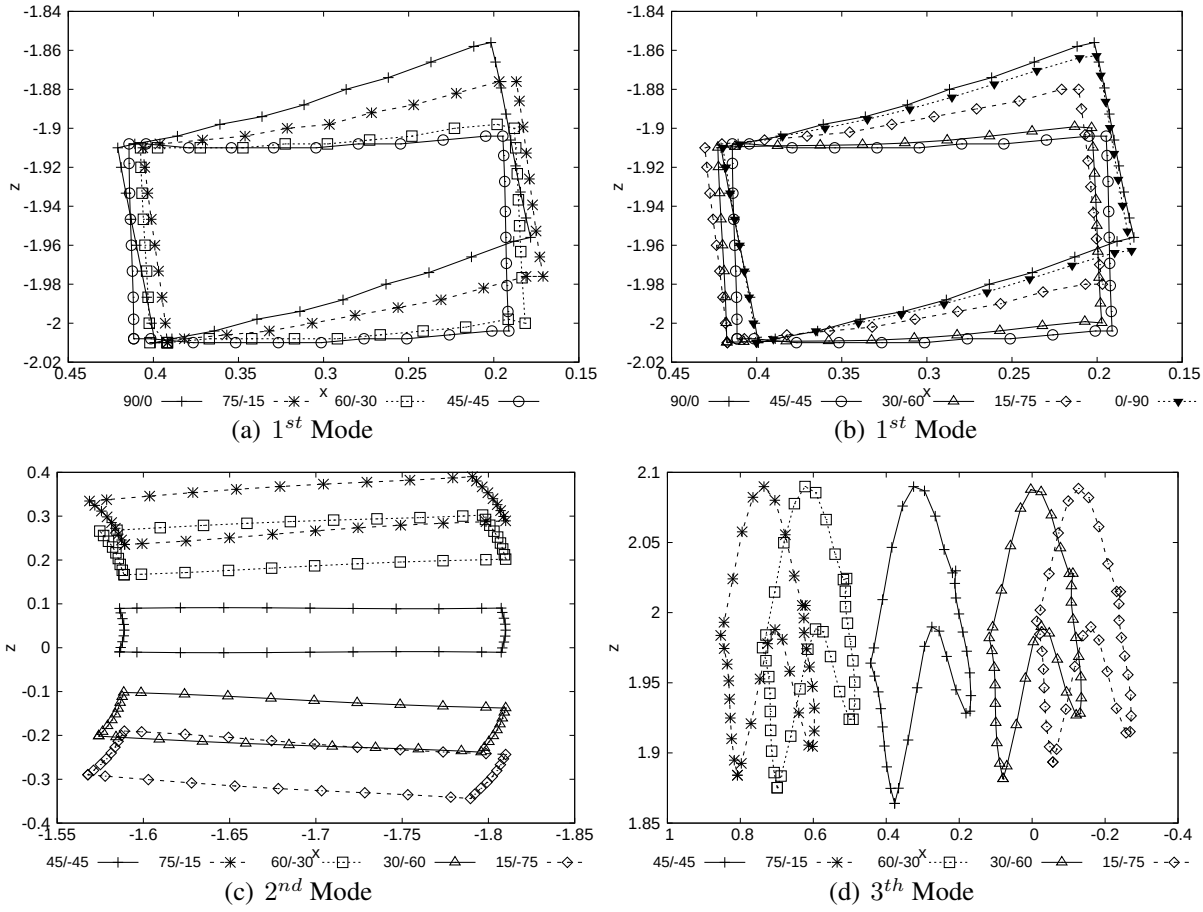

(a) 1^{st} Mode (b) 1^{st} Mode

(c) 2^{nd} Mode (d) 3^{th} Mode

Figure 8: Deformation of the tip with different lamination.

CONCLUSIONS

In this work the modal behaviour of tapered thin-walled boxes is investigated using a refined 1-D model derived in the framework of the Carrera Unified Formulation. The study is performed with structures made of a 2-ply laminate. The first 10 modes of a tapered box with no sweep angle are evaluated. Three different type of lamination are considered and the difference in the frequencies and in modal shapes are presented. In the second structure the tapered shape is limited to the horizontal panels and a sweep angle is introduced. In this case the lamination varying in a range of 180° maintaining a 90° angle between the two layer of the composite. Considerations are made on the first four frequency in terms of frequencies and modal shapes. The results provide some main remarks:

- This 1-d model correctly detects the modal behaviour of thin walled structures and detects shell-like modal shapes too;
- the performed analyses show good values of frequencies compared with those obtained from a shell model of a commercial code;
- using the layer-wise approach each layer can be separately individuated and the lamination can be defined at the layer level;
- as expects, the lamination deeply influences the behaviour of the structure, and the present model is able to detect the alterations.

In short, the present models can be used as an accurate tool in the design process and in the definition of a lay-up that can satisfy the requirements.

REFERENCES

[1] L. Euler. De curvis elasticis. Methodus inveniendi lineas curvas maximi minimive proprietate gaudentes, sive solutio problematis iso-perimetrici lattissimo sensu accepti. 1744.

[2] P. Cicala. *Sulle travi di altezza variabile*. Laboratorio di Aeronautica, Tipografia Vincenzo Bona, Turin, Italy, 1939.

[3] S.P. Timoshenko and J.N. Goodier. *Theory of elasticity*. McGraw-Hill, 1970.

[4] Ji Yao Shen, Elias G. AbuSaba, William M. McGinley, Jr. Lonnie Sharpe, and Jr. Lawrence W. Taylor. Continuous dynamic model for tapered beamlike structures. *Journal of Aerospace Engineering*, 7(4):435–445, 1994.

[5] M.J. Turner, R.W. Clough, H.C. Martin, and L.J. Topp. Stiffness and Deflection Analysis of Complex Structures. *Journal of the Aeronautical Sciences*, 23(9):805–823, sep 1956.

[6] E.F. Bruhn. *Analysis and design of flight vehicle structures*. Tri-State Offset Company, 1973.

[7] V.Z. Vlasov. *Thin walled elastic beams*. 1961.

[8] E Carrera, Cinefra M., M. Petrolo, and E Zappino. *Finite Element Analysis of Structures Through Unified Formulation*. John Wiley & Sons, 2014.

[9] E. Carrera, G. Giunta, P. Nali, and M. Petrolo. Refined Beam Ele-ments With Arbitrary Cross-Section Geometries. *Comput. Struct.*, 88(5–6):283–293, 2010.

[10] E. Carrera and M. Petrolo. Refined Beam Elements With Only Displacement Variables and Plate/Shell Capabilities. *Meccanica*, 47(3):537–556, 2012.

[11] E. Carrera, M. Filippi, and E. Zappino. Laminated Beam Analysis by Polynomial, rigonometric, Exponential and Zig-Zag Theories. *European Journal of Mechanics - A/Solids*, 41:58–69, 2013.

[12] S.W. Tsai. *Composites Design*. Dayton, Think Composites, 4th edition, 1988.

[13] J.N. Reddy. *Mechanics of laminated composite plates and shells. Theory and Analysis*. CRC Press, 2ˆ{nd} edition, 2004.

[14] E. Carrera, A. Pagani, and M. Petrolo. Classical, Refined and Component-wise Theories for Static Analysis of Reinforced-Shell Wing Structures. *AIAA Journal*, 51(5):1255–1268, 2013.

[15] Pagani A. Carrera E. and Petrolo M.. Free Vibrations of Damaged Aircraft Structures by Component-Wise Analysis.. *AIAA JOURNAL*, 54(10):3091–3106, 2016.

[16] Viglietti A. Zappino E. and Carrera E.. The analysis of tapered structures using a component-wise approach based on refined one-dimensional models. 65:141–156, 2017.

COPYRIGHT STATEMENT